RESEARCH

Open Access

Comparison between diffusion-weighted magnetic resonance and positron-emission tomography in the evaluation of treated lymphomas with mediastinal involvement

Francesca Di Giuliano[1], Eliseo Picchi[2,3]* , Noemi Pucci[2], Silvia Minosse[2], Valentina Ferrazzoli[2,3], Giulia Pizzicannella[2], Cecilia Angeloni[2], Daniela Nasso[3], Agostino Chiaravalloti[3], Francesco Garaci[3,4] and Roberto Floris[2,3]

Abstract

Background: The persistence of residual tissue after treatment is frequent in patients with mediastinal lymphomas and it is often characterized by ^{18}F-Flurodeoxyglucose Positron Emission Tomography (^{18}F-FDG PET) uptake. This study aims to investigate the usefulness of diffusion-weighted whole-body imaging with background body signal suppression (DWIBS) sequence in residual tissues of treated mediastinal lymphomas and to compare it with ^{18}F-FDG PET-CT.

Results: We included 21 patients with mediastinal Hodgkin and non-Hodgkin lymphomas who showed residual masses on PET-CT imaging at end of treatment and underwent DWIBS-Magnetic Resonance Imaging (MRI). SUV_{max} and Apparent Diffusion Coefficient (ADC) values of residual masses were assessed quantitatively, including measurement of mean ADC. 15 patients showed radiotracer uptake at ^{18}F-FDG PET-CT, among them only 3 had positive DWIBS-MRI with low ADC values (median value: 0.90 mm^2/s). The mediastinal biopsy in these 3 "double positive" patients confirmed pathological residual tissue. All the patients with positive ^{18}F-FDG PET-CT but negative DWIBS-MRI ($n = 18$) with high ADC values (median value: 2.05 mm^2/s) were confirmed negative by biopsy.

Conclusions: DWIBS-MRI examination combined with ADC measurement allowed to discriminate pathological and non-pathological residual tissue in patients with treated mediastinal lymphoma. These preliminary results seem to pave the way for a leading role of the MRI which could be a useful alternative to the ^{18}F-FDG PET/CT.

Keywords: Mediastinal lymphoma, Response assessment, Magnetic resonance imaging, DWIBS, ^{18}F-FDG PET/CT

Background

The mediastinum is involved approximately in 60% of systemic Hodgkin Lymphomas (HL) and in 20% of Non-Hodgkin Lymphomas (NHL) [1–6]; on the other hand, primary mediastinal lymphoma (PML) is quite rare (only 5–10% of the cases) with a prevalence of NHL (65%) type [2, 3, 5].

Computed Tomography (CT) is commonly used for the initial staging in lymphomas, although the current Lugano Classification recommends the use ^{18}F-Flurodeoxyglucose Positron Emission Tomography with Computed Tomography (^{18}F-FDG PET-CT) for staging and response assessment in ^{18}F-FDG-avid lymphomas, whereas the use of CT is indicated only for the ^{18}F-FDG non-avid indolent NHL subtypes [7–9].

*Correspondence: eliseo.picchi@hotmail.it

[2] Diagnostic Imaging Unit, Department of Biomedicine and Prevention, University of Rome Tor Vergata, Viale Oxford 81, 00133 Rome, Italy
Full list of author information is available at the end of the article

Standard treatment is strictly related to the histological subtype and usually includes systemic chemotherapy with or without radiotherapy consolidation depending on the extent of the disease [10, 11]. The persistence of mediastinal residual tissue after treatment is not infrequent and it is often characterized by ^{18}F-FDG uptake [12], ranging from 25 to 100% [13].

The persistent high metabolism in treated residual masses is mainly related to inflammatory changes and necrosis induced by treatments [14–16]; in case of radiotherapy, metabolic alterations may persist up to 3–4 months, precluding a precise determination as to the neoplastic nature of the residual tissue [17]. Moreover, the presence of mediastinal structures, as thymic hyperplasia or thymic regrowth following chemotherapy in young adults, can easily confuse the residual neoplastic tissue evaluation [16, 18].

The detection of residual disease in anterior mediastinal lymphomas is a pivotal issue because it has important therapeutic implications. To now, mediastinal biopsy remains the gold standard to establish definitive diagnosis [7, 8, 16, 18]. However, biopsies are reported to have low diagnostic accuracy due to the heterogeneity of the residual tissue after treatment composed of inflamed and fibrotic tissue [19]. Moreover, a mediastinal biopsy is an invasive procedure that requires general anaesthesia and is associated with significant risk due to the often small mass size and the proximity to anatomical structures such as the heart and great vessels.

To improve post-treatment response assessment, other instrumental investigations, such as diffusion weighted magnetic resonance imaging (DW-MRI), may be added. Actually, DW-MRI is a promising radiation-free technique for staging and following-up many types of neoplasms including lymphomas [20–24].

Diffusion-weighted whole-body imaging with background body signal suppression (DWIBS) is a DWI technique that can be used for the whole body evaluation producing PET-like images [25]. Over the past few years, DWIBS has revealed great potential in oncologic radiology and proved to be a radiation-free alternative to ^{18}F-FDG PET-CT [25–28].

The aim of this study is to assess the role of DWIBS-MRI compared to ^{18}F-FDG PET-CT in the definition/evaluation of residual tissue in treated mediastinal lymphomas to avoid/reduce the need of diagnostic biopsy.

Methods

Study design and patient enrolment

Inclusion criteria were patients with age of 18 years or more, diagnosed with mediastinal involvement of HL or NHL showing residual tissue at ^{18}F-FDG PET-CT after treatment (chemotherapy or chemotherapy with radiotherapy). The response assessment in PET (positive or negative) was carried out visually and quantitatively. The patients were classified in responder and not-responder according to Deauville Score (DS).

All participants underwent DWIBS-MRI examination, performed within a short time from ^{18}F-FDG PET-CT, with a median of 10 days (95% CI, 8–13 days). In patients treated also with radiotherapy the acquisition of imaging studies were performed four months after the end of treatment to minimize the impact of confounding factors such as inflammatory changes.

All patients gave a written informed consent to undergo ^{18}F-FDG PET.CT and DWIBS-MRI examination.

Exclusion criteria were absolute contraindications to MRI examination and to gadolinium-based contrast agent administration in accordance with European Society of Urogenital Radiology (ESUR) guidelines.

In all cases with suspicious mediastinal active disease a biopsy was planned to assess tissue composition.

The hospital ethics committee approved this study.

Magnetic resonance imaging protocol

All the patients underwent MRI after ^{18}F-FDG PET-CT. All MRI examinations were performed using a 1.5T scanner (Intera, Philips Medical System, Best, The Netherlands) equipped with a 12-channel phased-array body coil.

The MRI protocol included: T2 Turbo Spin Echo (T2 TSE) on the axial plane (acquisition matrix 320×282, repetition time/echo time (TR/TE) 500 ms/100 ms, slice thickness: 5 mm); T2 TSE with Spectral Presaturation Inversion Recovery (SPIR) on the axial plane (acquisition matrix 320×282, repetition time/echo time (TR/TE) 500 ms/100 ms, slice thickness: 5 mm); T1 Dual Fast Field Echo (dual FFE) on the axial plane (acquisition matrix 280×280, TR/TE 205 ms/2.3 ms, slice thickness: 5 mm; flip angle 75°). DWI was performed with DWIBS technique using an echo planar imaging (EPI) during free breathing with the following parameters: TR/TE 5423 ms/80 ms, slice thickness: 4 mm, voxel size 3.5×3.5 mm^2. Two different *b* values ($b=0$ and 800 s/mm^2) were used, with all diffusion-sensitizing gradients applied in three orthogonal directions to obtain trace-weighted images. Each of the listed sequences was equipped with parallel acquisition technique (sensitivity encoding, SENSE), which is responsible for reaching an increased spatial resolution and decrease acquisition time.

During the administration of gadolinium-based contrast agent, dynamic axial and coronal mDIXON sequences were acquired (acquisition matrix 220×223, TR/TE 5 ms/0 ms, slice thickness 4 mm, flip angle 15°). Total MRI examination time was approximately 15 min.

Di Giuliano *et al. Egypt J Radiol Nucl Med*   (2022) 53:149

Page 3 of 9

ADC analyses

The Apparent Diffusion Coefficient (ADC) maps were obtained using a commercial software package (IntelliSpace Portal 9.0 clinical applications MR Diffusion, Philips) including DWIBS with two different b values ($b = 0$ and 800 s/mm^2). A region of interest (ROI) was manually defined by two radiologists in consensus with > 5 years of experience in MRI. 3D Slicer Software [29] was used for images visualization and for tumor segmentation. The two radiologists didn't have access to other examinations, or original reports and didn't know the PET-CT results.

PET imaging protocol

^{18}F-FDG PET-CT was performed, from the vertex to the upper thigh, using a 64-row multidetector PET/CT system (Biograph True Point 64; Siemens), with a trans-axial field of view (FOV) of 605 mm (axial FOV, 216 mm), a PET sensitivity of 7.6 cps/kBq and a trans-axial PET resolution of 4 to 5 mm (full width at half maximum). Patients fasted for 5 h before imaging; the glucose cut-off level was 150 mg/dL. PET was performed 50–60 min after a weight-dependent intravenous administration of 18F FDG (target dose, 300 MBq; individual dose, 270–340 MBq), with 3 min/position read, four iterations for 21 subsets, a 5 mm thick slice and one 168×168 matrix, using the TrueX reconstruction algorithm. The portal venous phase of contrast-enhanced CT was obtained after intravenous injection of 100 mL of organo-iodinated contrast medium at a rate of 2 mL/s; the tube voltage was 120 kV, tube current of 230 mA, collimation of 64×0.6 mm, a slice thickness of 3 mm with an increment of 2 mm and a 512×512 matrix.

Maximum standardized uptake analysis

Maximum standardized uptake value (SUV$_{max}$, g/mL) was calculated using the standard formula.

SUV = tissue uptake/(injected FDG dose/patient weight), as proposed by Weber et al. [30], on a dedicated workstation (advantage workstation 4.4. GE medical systems) for all the PET/CT examinations, by one experienced nuclear medicine physician. A volume of interest (VOI) was drawn on fused PET/CT images including the residual mediastinal pathologic tissue around the slice that showed the highest uptake of 18F-FDG. When necessary, co-registered CT images were used for a correct VOI placement.

Statistical analysis

The variables were reported as absolute frequencies and percentages for categorical variables and median and 95% CI for continuous variables. The difference among groups was evaluated applying univariate analysis by nonparametric test (Fisher's exact test in case of categorical variables, Mann–Whitney U test in case of continuous variables).

Two boxplots were used to show, respectively, the ADC and the SUV values during the follow-up evaluation.

Spearman's Ranked Correlation test was used to investigate the correlation between two parameters (SUV$_{max}$ and ADC). Correlation coefficients are considered to represent a small effect from 0.1 to 0.3, a medium effect from 0.3 to 0.5, and a large effect if greater than 0.5 [31].

A p-value < 0.05 was considered statistical significative.

All analyses were performed using MATLAB software version 9.7.0, release 2019b (MathWorks, Natick, MA, USA).

Results

21 consecutive patients diagnosed with HL and NHL were enrolled in this study (from June 2017 until May 2021) with a median follow-up of 18 months (12–47 months). The patients were 8 males and 13 females, with a median age of 36 years (range: 25–47). According to World Health Organization (WHO) classification 12 patients were diagnosed with HL and 9 with NHL, with the last including 8 primary mediastinal B-cell lymphomas (PMBL) and 1 Diffuse Large B-Cell Lymphoma not otherwise specified (DLBCLnos). The patients' clinical and demographic characteristics are reported in Table 1.

The Ann Arbor Classification staging at onset of disease showed 3 patients with an extra-nodal localization 18 patients received chemotherapy plus radiotherapy and 3 patients received only chemotherapy.

The measurement of post therapy-residual mass showed only 2 patients with a residual mediastinal bulky mass (patient 1 and patient 21).

All 21 patients were divided into two groups for each imaging technique: PET/CT-positive ($n = 15$, 71.4%) and PET/CT-negative ($n = 6$, 28.6%) patients; MRI-positive ($n = 3$, 14.3%) and MRI-negative ($n = 18$, 85.7%) patients (Table 2). A statistically significant difference between the two groups of each imaging technique was found ($p < 0.001$).

We used a cut-off of DS 3 and 4, which corresponds to the background uptake in the liver, to distinguish between negative and positive PET/CT scan [32].

We applied an ADC cut-off value of 1.21×10^{-3} mm^2/s, that was reported to increase specificity for residual nodal disease detection by nearly 30% compared to visual inspection by Littooij et al. [33].

SUV$_{max}$ values derived from PET-CT and ADC values derived from DWIBS sequences are illustrated in Table 3. In the PET-positive group, SUV$_{max}$ values of

Di Giuliano *et al. Egypt J Radiol Nucl Med*   (2022) 53:149

Page 4 of 9

Table 1 Patients' clinical and demographic characteristics

ID	Gender	Age	Histology (WHO)	Ann Arbor classification at onset	Treatment	Post-therapy residual mass (cm)*
1	F	36	HL	2B	Chemo + RT	5 × 3
2	F	46	HL	2B	Chemo + RT	2 × 1.7
3	M	45	HL	2A	Chemo + RT	3 × 1
4	M	54	HL	2B	Chemo + RT	7 × 4
5	F	33	PMBL	2B	Chemo + RT	4 × 1.5
6	M	36	HL	2A	Chemo + RT	3.5 × 2.6
7	F	27	HL	2B	Chemo + RT	4 × 3
8	M	25	HL	2B	Chemo + RT	7.7 × 5.8
9	F	30	HL	3B	Chemo	5 × 2.8
10	F	36	HL	2B	Chemo + RT	2 × 2
11	F	37	PMBL	2B	Chemo + RT	5 × 9
12	F	37	PMBL	2B	Chemo + RT	4 × 5
13	F	43	PMBL	2B	Chemo + RT	2 × 0.8
14	F	30	HL	2B	Chemo + RT	5 × 4
15	F	47	PMBL	3B	Chemo + RT	2 × 1.4
16	F	28	HL	2A	Chemo	1.4 × 1.7
17	M	38	HL	2B	Chemo + RT	1.7 × 3
18	F	29	PMBL	4B (lung)	Chemo + RT	1 × 1
19	F	25	HL	4B (liver)	Chemo	3.4 × 3
20	M	30	PMBL	4B (lung, liver)	Chemo	5 × 2
21	M	45	DLBCLnos	3B	Chemo	12 × 3

M male; *F* female; *HL* hodgkin lymphoma; *PMBL* primary mediastinal (Thymic) B-cell lymphoma; *DLBCLnos* diffuse large B-Cell lymphoma not otherwise specified; *Chemo* chemotherapy, *RT* radiotherapy

*Measures in cm of the two largest diameters

Table 2 Summary results of instrumental methods examined (PET/CT and MRI)

Result	Positive	Negative	*p*-value
PET/CT	15 (71.4%)	6 (28.6%)	$p < 0.001$
MRI	3 (14.3%)	18 (85.7%)	$p < 0.001$

p-value: Fisher's Exact test $p < 0.05$ significant

Table 3 SUV_{max} and ADC values

Result	Positive	Negative	*p*-value
SUV_{max}	3.00 [2.65–4.65]	1.90 [1.70–2.20]	$p = 0.001$
ADC [mm^2/s]	0.90 [0.80–1.20]	2.05 [1.70–2.40]	$p = 0.008$

Values: median 95%CI; *p*-value: Mann–Whitney test $p < 0.05$ significant

the residual tissues were significantly higher compared to PET-negative one ($p = 0.001$). In the MRI-positive group, ADC values were significantly lower compared to MRI-negative patients ($p = 0.008$). Box plots of SUV_{max} and ADC are showed in Fig. 1.
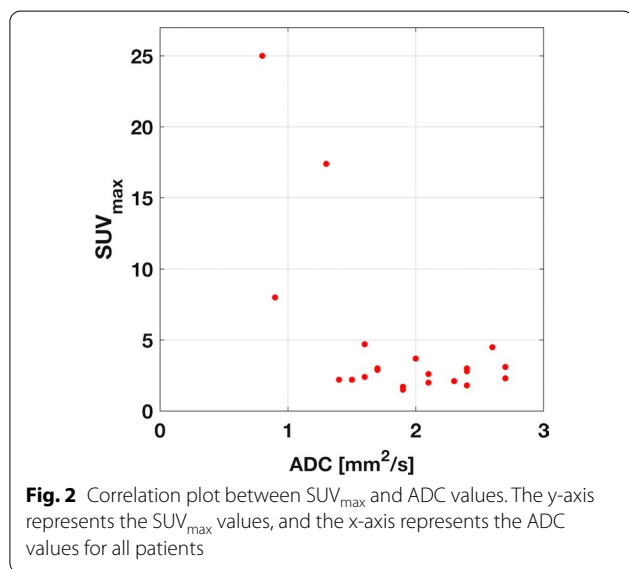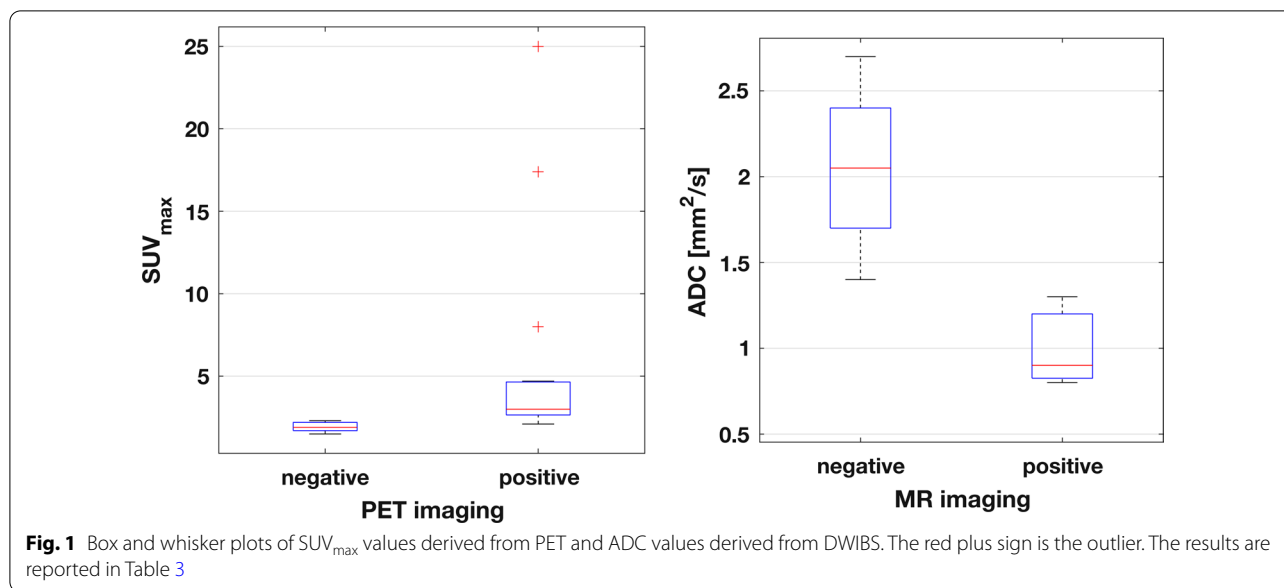
The Spearman's Ranked Correlation between SUV_{max} and ADC was not statistically significant (rho = − 0.289, $p = 0.204$) (Fig. 2).

Among the 15 PET/CT-positive patients (DS 4-5), 3 of them (*n*. 14, 19, 21) were also considered MRI-positive (PET+/MRI+ and all 3 had high SUV_{max} values (8; 17.4; 25) and low ADC values (0.9; 1.2; 0.8) with a median value of 0.90 mm^2/s (Fig. 3): due to the high radiological suspicion of residual disease these 3 patients underwent to mediastinal biopsy for histological confirmation. All mediastinal biopsies were positive for active disease.

The 12 remaining PET/CT-positive and MRI-negative (PET+/MRI−) patients and were confirmed negative by biopsy (Fig. 4).

The 6 patients with negative PET/CT (DS 1-3) had also negative MRI (PET-/MRI-), with high ADC values (median value of 2.05 mm^2/s) and underwent a clinical/laboratoristic follow-up. With a median follow-up of 18 months, none of the 18 MRI-negative patients presented any evidence of disease recurrence.

We analysed for each patient the signal enhancement curves in specific ROI but no significant correlation with ADC values was found.

Fig. 1 Box and whisker plots of SUV$_{max}$ values derived from PET and ADC values derived from DWIBS. The red plus sign is the outlier. The results are reported in Table 3

Fig. 2 Correlation plot between SUV$_{max}$ and ADC values. The y-axis represents the SUV$_{max}$ values, and the x-axis represents the ADC values for all patients

Discussion

The present pilot study focused on the ability of MRI with DWIBS sequence to assess disease activity in residual tissue of treated mediastinal lymphomas.

Specifically, our study focused on differentiating pathological from non-pathological residual tissue using quantitative measurements of ADC values, with the aim to reduce unnecessary invasive biopsy. Nowadays, mediastinal biopsy is still requested to establish disease presence in patients with suspicious metabolic activity of residual masses on ^{18}F-FDG PET-CT examination [7, 8].

Our results showed that high ADC values had a significant association with the absence of residual disease in patients with mediastinal lymphoma after treatment. High ADC values on DWIBS-MRI have been reported in all the 18 patients that were confirmed negative for residual disease; in these patients' median ADC values was 2.05 mm^2/s. At the same time, ^{18}F-FDG PET/CT showed mild persistent metabolic activity in 12 of these 18 cases (Table 3). These results showed that ADC measurement has a good capacity to detect the absence of disease in residual tissues in this group of patients, according with other studies [33, 34].

On the other hand, residual pathological tissues, confirmed at histology after mediastinal biopsy, were characterized by very high SUV$_{max}$ at ^{18}F-FDG PET/CT and low ADC values (≤ 1.2 mm^2/s).

In recent years, several studies have confirmed the ability of DWI to detect and distinguish malignancies from benign tissue, showing that ADC values are inversely correlated with cell density: for this reason DWI has been proposed for diagnosis, staging and evaluation of therapeutic response of various malignancies, including lymphomas [34–41].

Mayerhoefer and colleagues [24] reported that DW-MRI may be a useful alternative technique to ^{18}F-FDG PET/CT for treatment response assessment in patients with lymphoma allowing for highly reliable identification of complete or partial remission, stable and progressive disease. Moreover, DW-MRI might have some advantages over ^{18}F-FDG PET-CT as the latter suffers from a high number of false-positive after therapy primarily caused by inflammatory changes [14, 15, 42–44].
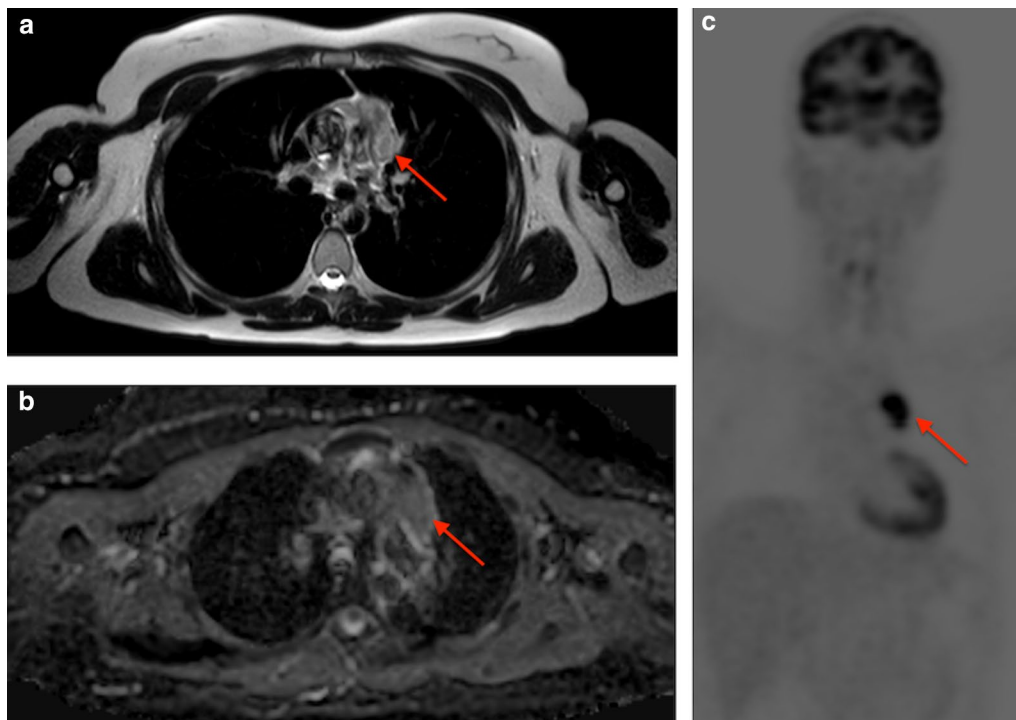
Fig. 3 30-years-old female affected by HL with anterior mediastinal residual mass after therapeutic treatment. MRI showed a tissue with inhomogeneous signal intensity on T2-weighted images **a** and low values on apparent diffusion coefficient (ADC) map, related to hypercellularity (ADC: 1.3×10^{-3} mm^2/s) (**b**). 18F-FDG- PET/CT showed an avid anterior mediastinal mass (SUV$_{max}$: 17.4) (**c**). Active residual disease was confirmed by histopathological evaluation

However, incongruent findings on DWI evaluation of residual tissue have been reported when visual DWI analysis was used; a better and more homogenous correlation between ADC values and residual disease was found when quantitative ADC evaluations were performed [33]. In this regard, Littooij et al. [33] investigated the diagnostic performance of whole-body DW-MRI, including ADC measurements, for the detection of residual disease in various types of treated lymphoma with different localizations. They showed that ADC could be a valuable adjunct for the discrimination between pathological and non-pathological residual lesions.

The introduction of DWIBS techniques has increased the diagnostic capabilities of MRI. DWIBS is an EPI pulse sequence offering heavy diffusion weighting and enhanced Short TI Inversion Recovery (STIR) with fat suppression using free-breathing with the result of reduced scan times, less DWI-specific (like magnetic susceptibility) and movement artifacts with good quality examinations [25, 45]. These features are especially important to study anatomic regions that are affected by respiration movement artefact, such as the mediastinum. In recent years an increasing number of studies has been published showing that DWIBS can be a valid

radiation-free alternative to ^{18}F-FDG PET/CT technique for treatment response assessment in lymphoma and it can be useful to prevent radiation long-term side-effects especially in young patients [27, 28, 33, 34].

To our knowledge, only a previous study focused on the role of DW-MRI in the evaluation of the specific group of mediastinal lymphomas, asserting that DWI is a valid and promising technique for the diagnosis and therapy response assessments in these patients [46]. This trial included only two cases with a residual mediastinal mass after treatment, and unlike our study it did not evaluate the tissue metabolic activity by ^{18}F-FDG PET/CT [46].

In our study, 15 of 21 patients showed uptake on ^{18}F-FDG PET/CT examination; however only 3 of them were considered "MRI-positive" (PET+/MRI+ with low ADC values and the biopsy confirmed the presence of pathological residual tissue. The remaining 12 cases had high ADC values and were considered MRI-negative (PET+/MRI−); these patients were confirmed negative by biopsy and thereby considered as false-positive cases at ^{18}F-FDG PET/CT.

Our results are in accord with those found in a recent review reporting a proportion of false-positive results ranging from 7.7 to 90.5% among all biopsied FDG-avid lymphoma at ^{18}F-FDG PET-CT performed during or after
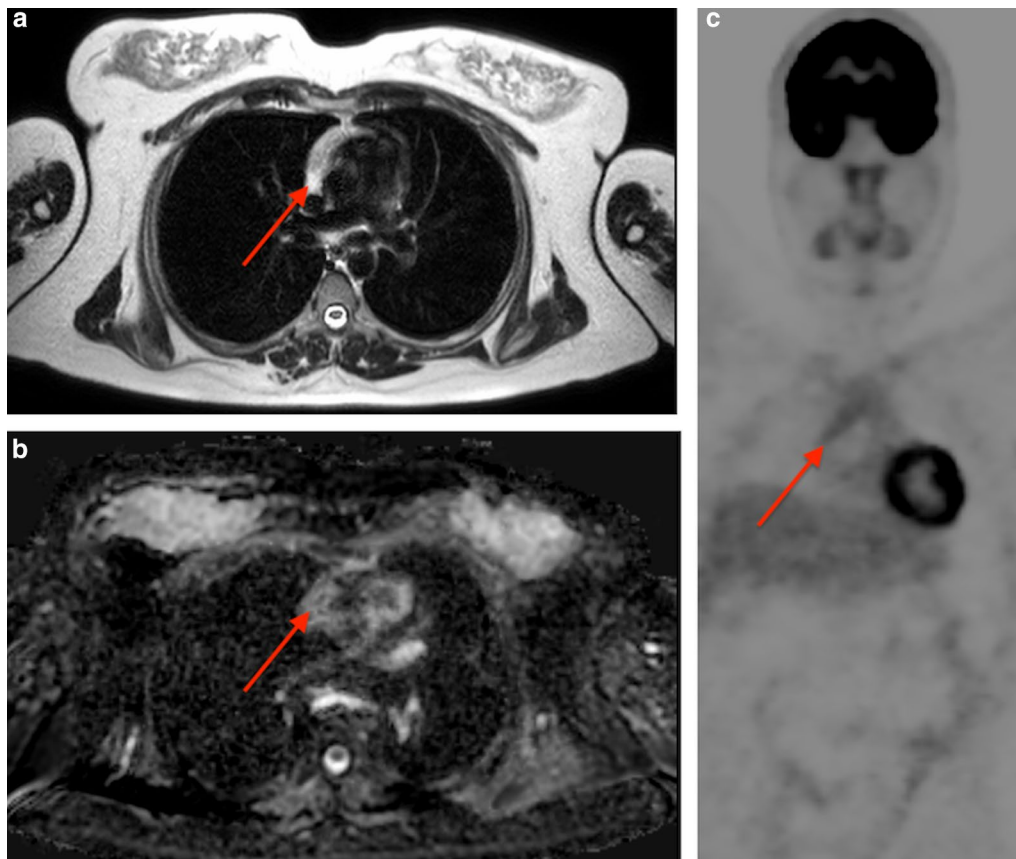
Fig. 4 25-years-old female affected by HL with anterior mediastinal residual mass after therapeutic treatment. T2-weighted images showed an hyperintense tissue **a** which presented also a mild hyperintensity on apparent diffusion coefficient (ADC) map (ADC: 1.6×10^{-3} mm^2/s) (**b**). 18F-FDG- PET/CT showed moderately increased metabolic activity (SUV_{max}: 4.7) (**c**). Biopsy demonstrated no disease progression

completion of treatment [15]; therapy-induced inflammatory changes are considered the mainly responsible of these results [15, 16].

According to Novo et al. [13], a DS of 3 and 4 may be ambiguous and unreliable in predicting persistent disease in mediastinal residual mass after therapy, as 50% of biopsies that they performed in these cases were negative.

According to Giraudo et al. [47], we did not find statistical significant correlation between ADC and SUV values.

Our MRI protocol included also dynamic post-contrast sequences. We analysed for each patient the signal-intensity time curves in specific ROI but no significant correlations with ADC values were found. Although DCE-MRI is not necessary it can be a valuable adjunct to give more information about tissue vascularization, helping to differentiate between residual or recurrent tumour and post-treatment changes (e.g., fibrosis).

Our study has some limitations. First, a main limitation is represented by the small number of enrolled patients: however, we feel that this limitation could be partially overtaken by the relative group homogeneity. As matter of fact, most of the other studies that evaluated the same techniques enrolled patients affected by several types of lymphoma with different localizations.

In addition, a limitation is related to the lack of a pre-treatment MRI, which could have been useful to compare the tissue ADC value before and after treatment considering the different features of "inflammatory" background on the histopathological examination of each lymphoma.

Conclusions

The results of our study show that DWIBS-MRI can be a valid free-radiation alternative to ^{18}F-FDG PET/CT for therapy response assessment in mediastinal lymphomas with residual tissues, since a significant association was found between high ADC values and inactive residual tissues. Thereby DWIBS-MRI can be a promising technique to overcome ^{18}F-FDG PET-CT limitations. Larger studies are needed to establish the role of DWIBS-MRI in this group of patients.

Di Giuliano *et al. Egypt J Radiol Nucl Med*   (2022) 53:149

Page 8 of 9

Abbreviations

HL: Hodgkin lymphoma; NHL: Non-hodgkin lymphoma;; PML: Primary mediastinal lymphoma; PMBL: Primary mediastinal B-cell lymphoma; 18F-FDG-PET/CT: 18F-fluorodeoxyglucose-positron emission tomography/computed tomography; SUV_{max}: Maximum standard uptake value; MRI: Magnetic resonance imaging; DWI: Diffusion-weighted imaging; ADC: Apparent diffusion coefficient; DWIBS: Diffusion weighted whole body imaging with background body signal suppression; DS: Deauville score; STIR: Short TI inversion recovery.

Author contributions

All authors contributed to the study conception and design and read and approved the final manuscript. FDG contributed to the study conception and design, analysis and interpretation of data and drafting of the manuscript. EP contributed to the study conception, design and drafting of the manuscript. NP contributed to the drafting of the manuscript and acquisition of data. SM contributed to the analysis and interpretation of data. VF contributed to acquisition of data and critical revision of the manuscript. GP contributed to acquisition of MRI data acquisition and drafting of the manuscript. CA contributed to critical revision and English revision of the manuscript. DN was responsible for recruitment and acquisition of haematologic data. AC was responsible of PET data acquisition and contributed to critical revision of the manuscript. FG and RF contributed to the study conception and design, analysis and interpretation of data and critical revision of the manuscript. All authors read and approved the final manuscript.

Availability of data and materials

The data analyzed for this study are available from the corresponding author on request.

Declarations

Ethics approval and consent to participate

A written consent was obtained from each participant sharing in this study. The hospital ethics committee approved this study.

Consent for publication

All patients included in this research gave written informed consent to publish the data contained within this study.

Competing interests

All authors declare that they have no conflict of interest.

Author details

[1]Neuroradiology Unit, Department of Biomedicine and Prevention, University of Rome Tor Vergata, Viale Oxford 81, 00133 Rome, Italy. [2]Diagnostic Imaging Unit, Department of Biomedicine and Prevention, University of Rome Tor Vergata, Viale Oxford 81, 00133 Rome, Italy. [3]Department of Biomedicine and Prevention, University of Rome Tor Vergata, Via Montpellier 1, 00133 Rome, Italy. [4]San Raffaele Cassino, Via Gaetano di Biasio 1, 03043 Cassino, Italy.

References

1. Roman E, Smith AG (2011) Epidemiology of lymphomas. Histopathology. https://doi.org/10.1111/j.1365-2559.2010.03696.x
2. Temes R et al (1999) Primary mediastinal malignancies: findings in 219 patients. West J Med 170(3):161–166
3. Swerdlow AJ (2003) Epidemiology of Hodgkin's disease and non-Hodgkin's lymphoma. Eur J Nucl Med Mol Imaging. https://doi.org/10.1007/s00259-003-1154-9
4. Temes R, Allen N, Chavez T, Crowell R, Key C, Wernly J (2000) Primary mediastinal malignancies in children: report of 22 patients and comparison to 197 adults. Oncologist 5(3):179–184. https://doi.org/10.1634/theoncologist.5-3-179
5. Tateishi U et al (2004) Primary mediastinal lymphoma. J Comput Assist Tomogr 28(6):782–789. https://doi.org/10.1097/00004728-20041 1000-00009
6. Dabrowska-Iwanicka A, Walewski JA (2014) Primary mediastinal large B-cell lymphoma. Curr Hematol Malig Rep 9(3):273–283. https://doi.org/10.1007/s11899-014-0219-0
7. Barrington SF et al (2014) Role of imaging in the staging and response assessment of lymphoma: consensus of the international conference on malignant lymphomas imaging working group. J Clin Oncol 32(27):3048–3058. https://doi.org/10.1200/JCO.2013.53.5229
8. Cheson BD et al (2014) Recommendations for initial evaluation, staging, and response assessment of Hodgkin and non-Hodgkin lymphoma: the Lugano classification. J Clin Oncol 32(27):3059–3067. https://doi.org/10.1200/JCO.2013.54.8800
9. Cheson BD (2015) Staging and response assessment in lymphomas: the new Lugano classification. Chin Clin Oncol 4(1):5. https://doi.org/10.3978/j.issn.2304-3865.2014.11.03
10. Brusamolino E et al (1994) Early-stage Hodgkin's disease: long-term results with radiotherapy alone or combined radiotherapy and chemotherapy. Ann Oncol 5:S101–S106. https://doi.org/10.1093/annonc/5.suppl_2.S101
11. Zinzani PL et al (2009) Rituximab combined with MACOP-B or VACOP-B and radiation therapy in primary mediastinal large B-cell lymphoma: a retrospective study. Clin Lymphoma Myeloma 9(5):381–385. https://doi.org/10.3816/CLM.2009.n.074
12. Zinzani PL et al (2007) Histological verification of positive positron emission tomography findings in the follow-up of patients with mediastinal lymphoma. Haematologica 92(6):771–777. https://doi.org/10.3324/haematol.10798
13. Novo M et al (2020) Persistent mediastinal FDG uptake on PET-CT after frontline therapy for Hodgkin lymphoma: biopsy, treat or observe? Leuk Lymphoma 61(2):318–327. https://doi.org/10.1080/10428194.2019.1663422
14. Mena E et al (2014) A pilot study of the value of 18F-fluoro-deoxy-thymidine PET/CT in predicting viable lymphoma in residual 18F-FDG avid masses after completion of therapy. Clin Nucl Med 39(10):874–881. https://doi.org/10.1097/RLU.0000000000000539
15. Adams HJA, Kwee TC (2016) Proportion of false-positive lesions at interim and end-of-treatment FDG-PET in lymphoma as determined by histology: Systematic review and meta-analysis. Eur J Radiol 85(11):1963–1970. https://doi.org/10.1016/j.ejrad.2016.08.011
16. Kane L, Savas H, DeCamp MM, Bharat A (2018) Utility of minimally invasive thoracoscopy for assessment of residual mediastinal lymphoma. Surgery 164(4):825–830. https://doi.org/10.1016/j.surg.2018.05.039
17. Juweid ME et al (2007) Use of Positron emission tomography for response assessment of lymphoma: consensus of the imaging subcommittee of international harmonization project in lymphoma. J Clin Oncol 25(5):571–578. https://doi.org/10.1200/JCO.2006.08.2305
18. Zhen Z et al (2010) Clinical analysis of thymic regrowth following chemotherapy in children and adolescents with malignant lymphoma. Jpn J Clin Oncol 40(12):1128–1134. https://doi.org/10.1093/jjco/hyq149
19. Petranovic M et al (2015) Diagnostic yield of CT-guided percutaneous transthoracic needle biopsy for diagnosis of anterior mediastinal masses. Am J Roentgenol 205(4):774–779. https://doi.org/10.2214/AJR.15.14442
20. Fitzpatrick JJ, Ryan MA, Bruzzi JF (2018) Diagnostic accuracy of diffusion-weighted imaging- magnetic resonance imaging compared to positron emission tomography/computed tomography in evaluating and assessing pathological response to treatment in adult patients with lymphoma: a systematic review. J Med Imaging Radiat Oncol 62(4):530–539. https://doi.org/10.1111/1754-9485.12723
21. Patyk M et al (2018) Application of the apparent diffusion coefficient in magnetic resonance imaging in an assessment of the early response to treatment in Hodgkin's and non-Hodgkin's lymphoma–pilot study. Polish J Radiol 83:210–214. https://doi.org/10.5114/pjr.2018.76007
22. Lin C et al (2012) Whole-body diffusion magnetic resonance imaging in the assessment of lymphoma. Cancer Imaging 12(2):403–408. https://doi.org/10.1102/1470-7330.2012.9048

Di Giuliano *et al. Egypt J Radiol Nucl Med*   (2022) 53:149

Page 9 of 9

23. Padhani AR et al (2009) Diffusion-weighted magnetic resonance imaging as a cancer biomarker: consensus and recommendations. Neoplasia 11(2):102–125. https://doi.org/10.1593/neo.81328

24. Mayerhoefer ME et al (2015) Evaluation of diffusion-weighted magnetic resonance imaging for follow-up and treatment response assessment of Lymphoma: results of an 18F-FDG-PET/CT–controlled prospective study in 64 patients. Clin Cancer Res 21(11):2506–2513. https://doi.org/10.1158/1078-0432.CCR-14-2454

25. Takahara T, Imai Y, Yamashita T, Yasuda S, Nasu S, Van Cauteren M (2004) Diffusion weighted whole body imaging with background body signal suppression (DWIBS): technical improvement using free breathing, STIR and high resolution 3D display. Radiat Med 22(4):275–282

26. Nava D, de Oliveira HC, Luisi FA, Ximenes ARDS, Lederman HM (2011) Aplicação da ressonância magnética de corpo inteiro para o estadiamento e acompanhamento de pacientes com linfoma de Hodgkin na faixa etária infanto-juvenil: comparação entre diferentes sequências. Radiol Bras 44(1):29–34. https://doi.org/10.1590/S0100-398420110001000009

27. Baranska D et al (2019) Feasibility of diffusion-weighted imaging with DWIBS in staging Hodgkin lymphoma in pediatric patients: comparison with PET/CT. Magn Reson Mater Phys Biol Med 32(3):381–390. https://doi.org/10.1007/s10334-018-0726-4

28. Sun M et al (2018) Application of DWIBS in malignant lymphoma: correlation between ADC values and Ki-67 index. Eur Radiol 28(4):1701–1708. https://doi.org/10.1007/s00330-017-5135-y

29. Fedorov A et al (2012) 3D Slicer as an image computing platform for the Quantitative Imaging Network. Magn Reson Imaging. https://doi.org/10.1016/j.mri.2012.05.001

30. Weber WA, Ziegler SI, Thã R, Hanauske A, Schwaiger M (1999) Reproducibility of metabolic measurements in malignant tumors using FDG PET. J Nucl Med 40:1771–1777

31. Cohen J (2013) Statistical power analysis for the behavioral sciences. Routledge, Milton Park

32. Metser U, Mohan R, Beckley V, Moshonov H, Hodgson D, Murphy G (2016) FDG PET/CT response assessment criteria for patients with Hodgkin's and non-Hodgkin's lymphoma at end of therapy: a multiparametric approach. Nucl Med Mol Imaging 50(1):46–53. https://doi.org/10.1007/s13139-015-0368-7

33. Littooij AS et al (2015) Whole-body MRI-DWI for assessment of residual disease after completion of therapy in lymphoma: a prospective multicenter study. J Magn Reson Imaging 42(6):1646–1655. https://doi.org/10.1002/jmri.24938

34. Albano D et al (2016) Comparison between whole-body MRI with diffusion-weighted imaging and PET/CT in staging newly diagnosed FDG-avid lymphomas. Eur J Radiol 85(2):313–318. https://doi.org/10.1016/j.ejrad.2015.12.006

35. Gaur S, Turkbey B (2018) Prostate MR imaging for posttreatment evaluation and recurrence. Radiol Clin N Am 56(2):263–275. https://doi.org/10.1016/j.rcl.2017.10.008

36. Scherer M et al (2019) Early postoperative delineation of residual tumor after low-grade glioma resection by probabilistic quantification of diffusion-weighted imaging. J Neurosurg 130(6):2016–2024. https://doi.org/10.3171/2018.2.JNS172951

37. Tomura N et al (2006) Diffusion changes in a tumor and peritumoral tissue after stereotactic irradiation for brain tumors. J Comput Assist Tomogr 30(3):496–500. https://doi.org/10.1097/00004728-200605000-00024

38. Siegel MJ et al (2014) Diffusion-weighted MRI for staging and evaluation of response in diffuse large B-cell lymphoma: a pilot study. NMR Biomed 27(6):681–691. https://doi.org/10.1002/nbm.3105

39. Hagtvedt T et al (2015) Diffusion-weighted MRI compared to FDG PET/CT for assessment of early treatment response in lymphoma. Acta radiol 56(2):152–158. https://doi.org/10.1177/0284185114526087

40. Wu X et al (2011) Diffusion-weighted MRI in early chemotherapy response evaluation of patients with diffuse large B-cell lymphoma-a pilot study: comparison with 2-deoxy-2-fluoro- <scp>D</scp> -glucose-positron emission tomography/computed tomography. NMR Biomed 24(10):1181–1190. https://doi.org/10.1002/nbm.1689

41. Nural MS, Danaci M, Soyucok A, Okumus NO (2013) Efficiency of apparent diffusion coefficients in differentiation of colorectal tumor recurrences and posttherapeutical soft-tissue changes. Eur J Radiol 82(10):1702–1709. https://doi.org/10.1016/j.ejrad.2013.05.025

42. Hutchings M, Mikhaeel NG, Fields PA, Nunan T, Timothy AR (2005) Prognostic value of interim FDG-PET after two or three cycles of chemotherapy in Hodgkin lymphoma. Ann Oncol 16(7):1160–1168. https://doi.org/10.1093/annonc/mdi200

43. Terasawa T et al (2009) Fluorine-18-fluorodeoxyglucose positron emission tomography for interim response assessment of advanced-stage Hodgkin's lymphoma and diffuse large B-Cell lymphoma: a systematic review. J Clin Oncol 27(11):1906–1914. https://doi.org/10.1200/JCO.2008.16.0861

44. Barrington SF, O'Doherty MJ (2003) Limitations of PET for imaging lymphoma. Eur J Nucl Med Mol Imaging 30(S1):S117–S127. https://doi.org/10.1007/s00259-003-1169-2

45. Di Giuliano F et al (2020) Radiological imaging in multiple myeloma: review of the state-of-the-art. Neuroradiology 62(8):905–923. https://doi.org/10.1007/s00234-020-02417-9

46. Sabri YY, Ewis NM, Zawam HEH, Khairy MA (2021) Role of diffusion MRI in diagnosis of mediastinal lymphoma: initial assessment and response to therapy. Egypt J Radiol Nucl Med 52(1):215. https://doi.org/10.1186/s43055-021-00597-9

47. Giraudo C et al (2018) Correlation between glycolytic activity on [18F]-FDG-PET and cell density on diffusion-weighted MRI in lymphoma at staging. J Magn Reson Imaging 47(5):1217–1226. https://doi.org/10.1002/jmri.25884

Publisher's Note